Polymer 50 (2009) 2237–2245

Contents lists available at ScienceDirect

Polymer

journal homepage: www.elsevier.com/locate/polymer

The effect of thiol and ene structures on thiol–ene networks: Photopolymerization, physical, mechanical and optical properties

Qin Li, Hui Zhou, Charles E. Hoyle*

School of Polymers and High Performance Materials, The University of Southern Mississippi, Hattiesburg, MS 39406, United States

ARTICLE INFO

Article history:
Received 5 September 2008
Received in revised form
11 March 2009
Accepted 14 March 2009
Available online 25 March 2009

Keywords:
Thiol–ene
Secondary thiol
Structure–property relationship

ABSTRACT

The photopolymerization of four different types of ene monomers with both primary and secondary multifunctional thiols has been evaluated. To understand the effect of ene monomer structures on polymer properties, a comprehensive investigation of the basic physical, mechanical and optical properties was conducted for the secondary and primary thiol–ene networks. The results indicate that ene structure and functionality can significantly affect the rigidity and the physical and mechanical properties of the thiol–ene networks. The heat capacity in the rubber state correlates with the network crosslink density and flexibility of the ene component. Networks formed from the secondary thiol–ene systems are basically equivalent to those made from primary thiol–enes with respect to physical, mechanical and optical properties. The secondary thiol monomer samples evaluated were found to have exceptional storage stability and relatively low odor.

© 2009 Elsevier Ltd. All rights reserved.

1. Introduction

The photopolymerization of compounds having ethylenically unsaturated bonds, such as acrylates and methacrylates, often suffers from problems such as oxygen inhibition and insufficient curing [1,2]. The first issue is generally addressed by purging with inert gases or using high photoinitiator concentrations and/or high light intensities. One alternative is to expose a mixture of multifunctional thiols and multifunctional enes to light, leading to the formation of highly crosslinked networks with uniform structure in the presence of oxygen [1–4]. The photocured thiol–ene networks exhibit narrow glass transition regions and excellent mechanical and thermal properties. One of the attractive features of thiol–ene photopolymerization is that many types of enes and thiols can be incorporated into thiol–ene networks. The reactivity of three basic types of thiols, mercaptopropionate, thioglycolate and alkyl thiol, with various types of enes, such as norbornene, vinyl ether, allyl ether, allyl triazine, allyl isocyanurate, alkene, acrylate, methacrylate and styrene, has been reported in the literature [1,3,5,6]. There have been sporadic reports dealing with the kinetics of photocured thiol–ene networks and selected physical properties. However, there has not been a detailed evaluation of basic mechanical and thermal properties of thiol–ene systems as a function of ene structure.

Almost all of the thiols used in thiol–ene photopolymerization studies to date have been primary. Coincidentally, the shelf-life stability of these thiol–ene systems has been the subject of considerable concern. Possible reasons for the limited shelf-life of thiol–enes have been extensively studied and recently reviewed by Hoyle et al. [1,7–9]. In order to extend the shelf-life of thiol–ene mixture, numerous types of stabilizers, including sulfur, triallyl phosphates and the aluminum salt of N-nitrosophenylhydroxylamine have been used to prevent ambient thermal free-radical polymerization [10–14]. Recently there have been reports of photocurable thiol–enes based on a series of hindered multifunctional or secondary thiols, as depicted by the following structure

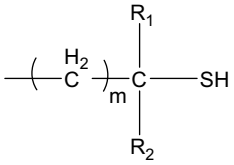

where R_1 is an alkyl group, such as a methyl or a phenyl group, and R_2 is either a H or an alkyl group [2,15–18]. A commercialized secondary thiol, pentaerythritol tetrakis(3-mercaptobutylate) (s-4T) (Chart 1), has been reported for use in numerous applications [15,17,19–24]. For example, Okamoto et al. added s-4T into a (meth)acrylate photocuring formulation to prepare antistatic hard coating films with excellent transparency [19]. Spacers, color filters and light sensitive coatings for liquid crystal displays were

* Corresponding author. Tel.: +1 601 266 5743; fax: +1 601 266 5504.
E-mail address: charles.hoyle@usm.edu (C.E. Hoyle).

0032-3861/$ – see front matter © 2009 Elsevier Ltd. All rights reserved.
doi:10.1016/j.polymer.2009.03.026

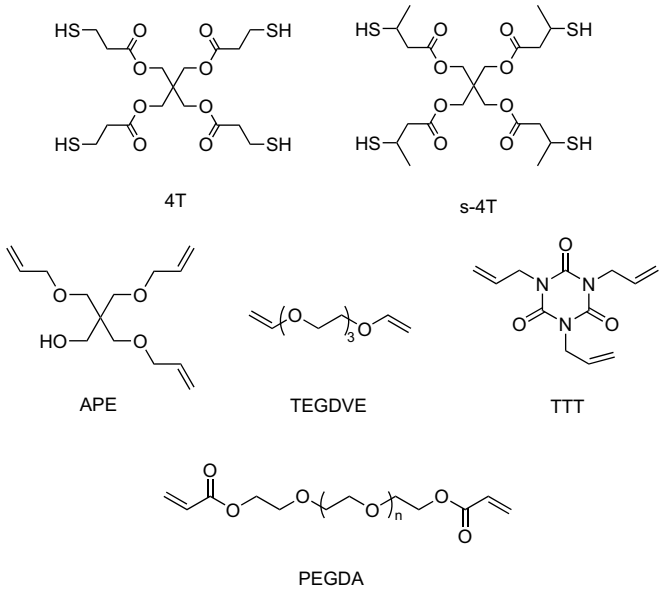

Chart 1. Chemical structures of thiols and enes.

also prepared from formulations containing secondary thiols and reported to exhibit excellent storage stability and photosensitivity [20–23]. Secondary thiols have also been produced as photocuring accelerators and for the preparation of thermally stable thiourethane containing photoinitiators [16,17]. Since thiol–ene resins composed of commercial secondary thiols have been reported to exhibit exceptional shelf-life stability [15,17–23], it is important to evaluate the properties of networks prepared from systems incorporating a commercial secondary thiol. To the best of our knowledge, there is almost no information about the properties of thiol–ene networks based on a commercial secondary thiol, let alone structure–property relationships.

Since it is important to understand physical properties of photocured thiol–ene networks in order to develop applications that combine a variety of essential properties, we decided to conduct a comprehensive investigation of a series of thiol–ene networks based on four different enes and both primary and secondary thiols. The photopolymerization of these enes with both primary and secondary thiols and the physical, mechanical and optical properties of the resultant thiol–ene films has been thoroughly characterized and analyzed, and basic structure–property relationships established.

2. Experimental

2.1. Materials

Pentaerythritol tetrakis(3-mercaptobutylate) (s-4T) was obtained from Showa Denko K.K. and used as received. Pentaerythritol triallyl ether (APE) was obtained from Perstorp and used as received. Polyethylene Glycol (400) Diacrylate (PEGDA) was obtained from Sartomer Chemical Company and used as received. The photoinitiator, 2,2-dimethoxy-2-phenylacetophenone (DMPA), was obtained from Ciba Specialty Chemical Company and used as received. Pentaerythritol tetrakis(3-mercaptopropionate) (4T), triallyl-1,3,5-triazine-2,4,6(1H, 3H,5H)-trione (TTT) and tri(ethylene glycol) divinyl ether (TEGDVE) were purchased from Aldrich Chemical Company and used as received.

2.2. Preparation

To prepare a thiol–ene film, 5.0 mmol of s-4T/4T, an equal molar double bond concentration of ene monomer (APE, TEGDVE, TTT) or a thiol/ene molar ratio of 20:80 (PEGDA), and 1 wt% of DMPA were charged into a clean 25 mL glass vial and mixed with the aid of sonication (the structures of all monomers are shown in Chart 1). The glass vial was completely wrapped with a layer of aluminum foil to prevent any prepolymerization. Once the photoinitiator was dissolved and homogeneously mixed, the formulation was evenly spread onto glass plates using a 5 mil (125 μm) draw down bar. Cured thiol–ene networks were obtained by exposing the coated glass or steel plates 10 times to the output of a Fusion high-intensity lamp system with conveyer belt (D bulb which is rich in UVA output (340–430 nm), 400 W/in. input, line speed of 3.05 m/min, light intensity of 3.0 W/cm^2). The thickness of the cured thiol–ene films was approximately 100 ± 20 μm. To prepare samples for shelf-life measurement, the formulations in the glass vials described above were wrapped with aluminum foil and stored in an ambient environment. It should be noted that the s-4T/4T–PEGDA samples used for shelf-life and real-time FTIR were equal molar mixtures of thiol and double bond.

2.3. Characterization

A modified Bruker IFS 99 FTIR spectrometer with a horizontal sample stage was used to monitor the photopolymerization of thiol and ene monomers and obtain real-time IR (RTIR) spectra [25–27]. UV light generated from an Oriel lamp system equipped with a high pressure mercury–xenon lamp (200 W) was delivered to the sample chamber through an optical fiber. The polymerization of thin layers of the above sample (~25 μm) sandwiched between two sodium chloride plates was initiated by continuous UV light irradiation within the sample chamber. The whole process was monitored by the FTIR spectrometer operating at 5 scans/s. The thermal properties of the prepared thiol–ene films were measured by a differential scanning calorimeter (DSC), TA Q1000 (TA Instruments) with the calorimetric precision (indium metal) of ±0.1%, operating at a heating rate of 10 °C/min. The second heating scan curves were used to determine the glass transition temperatures (T_g) by TA Universal Analysis software. The thermomechanical properties were measured with a TA Q800 DMA (TA Instruments) operating at 1 Hz and a heating rate of 3 °C/min (tensile mode). The modulus precision and isothermal stability of TA Q 800 are ±1% and ±0.1 °C, respectively. The peak maximum of the tan δ plot was taken as the glass transition temperature. The thermal stability of each thiol–ene network was measured with a TA Q50 (TA Instruments, Inc.) thermal gravimetric analysis (TGA) instrument with a weighing accuracy of ±0.1%, operating at a heating rate of 10 °C/min in N_2 atmosphere. Refractive index values with an accuracy of ±0.0001 were measured at 24 °C by a Bausch & Lomb ABBE-3L refractometer using a 589 nm light source. 1-Bromonaphthalene was applied between the sample film and the prism shield. The Persoz pendulum hardness values (average of six tests) were measured following ASTM D-4366 using a BYK-Gardner pendulum hardness tester with a square frame pendulum. The pencil hardness test was conducted according to ASTM D-3363 using graded pencil (from 9B to 9H) to scratch the coating surface at uniform velocity and force. The hardest pencil that produces no failure on a coating film was reported as the pencil hardness of the coating film.

3. Results and discussion

3.1. Shelf-life and polymerization kinetics

As has already been reported [15,17–23], resins prepared from secondary thiols exhibit excellent shelf-life stability. For reference, the shelf-life of all formulations was measured and the results are listed in Table 1. None of the secondary thiol–ene formulations

Table 1
Shelf-life of thiol–ene formulations (1 wt% DMPA) stored in dark and at room temperature.

	APE	TEGDVE	TTT	PEGDA
4T	15 days	12 h	10 days	9 days
s-4T[a]	Low η	Low η	High η	High η

[a] Stored for 20 days.

gelled after 20 days storage at room temperature, although the viscosity of the TTT and PEGDA based samples did increase, indicating the excellent thermal stability of these formulations. The primary thiol–enes evaluated are much less stable since all formulations gelled during the 20-day storage period. Particularly interesting, the mixture of 4T and TEGDVE, the very reactive vinyl ether monomer, gelled within 12 h while the s-4T–TEGDVE mixture had a low viscosity even after 20 days.

The polymerization kinetics of each of the thiol mixed with four different types of ene monomers was next measured by real-time FTIR at room temperature. For all four types of ene monomers, as shown in Fig. 1 the photopolymerizability of the samples with secondary thiol, s-4T, is not appreciably different than for the samples with primary thiol monomer, 4T, for the light intensity used. In reactions with APE and TEGDVE, both primary and secondary thiols show very fast polymerization rates. High conversions are attained since the glass transitions of the networks formed are well below room temperature (shown in next section). In cases of s-4T and 4T with TTT, high polymerization rates were also achieved, but with lower limiting conversions than for the systems with APE and TEGDVE under the experimental conditions (low light intensity of 0.625 mW/cm^2). As the three dimensional s-4T–TTT and 4T–TTT networks are formed, the glass transition temperature of the networks increases to greater than room temperature ($T_g \sim 45$ °C by DSC) hindering the further conversion of functional groups, i.e., diffusion limitation sets in under the irradiation conditions of low light intensity at room temperature. Fig. 1 shows that 1:1 molar functional group mixtures of 4T and s-4T with PEGDA are characterized by incomplete thiol functional group conversions. The conversion of thiol groups was greatly suppressed because of the high homopolymerization propensity of acrylate groups as indicated in Fig. 2. The acrylate monomer achieved complete double bond conversions within 50 s. We note that, in order to achieve high monomer conversion and eliminate the effect of unreacted monomers on polymer properties, a sample with only 20 mol% of thiol and 80 mol% of PEGDA was used to generate fully cured films for mechanical and physical testings.

3.2. Physical, mechanical and optical properties

From a practical point of view, it is important to characterize any effect of the thiol and ene structures on the physical properties of the photocured thiol–ene networks. Indeed the characterization of thiol–ene based networks has been amply characterized in the past with respect to structural parameters related to ene flexibility [1,28]. Basically it is well documented that thermal and mechanical parameters are directly related to features inherent to the chemical structure of both the thiol and ene functional groups. For instance, ring structures such as present in TTT will result in enhanced glass transition temperatures [1,28], and polyether groups such as found in TEGDVE result in lower glass transitions [29,30]. Furthermore, it has been shown that the functionality of both the ene and thiol will influence the crosslink density and glass transition temperature

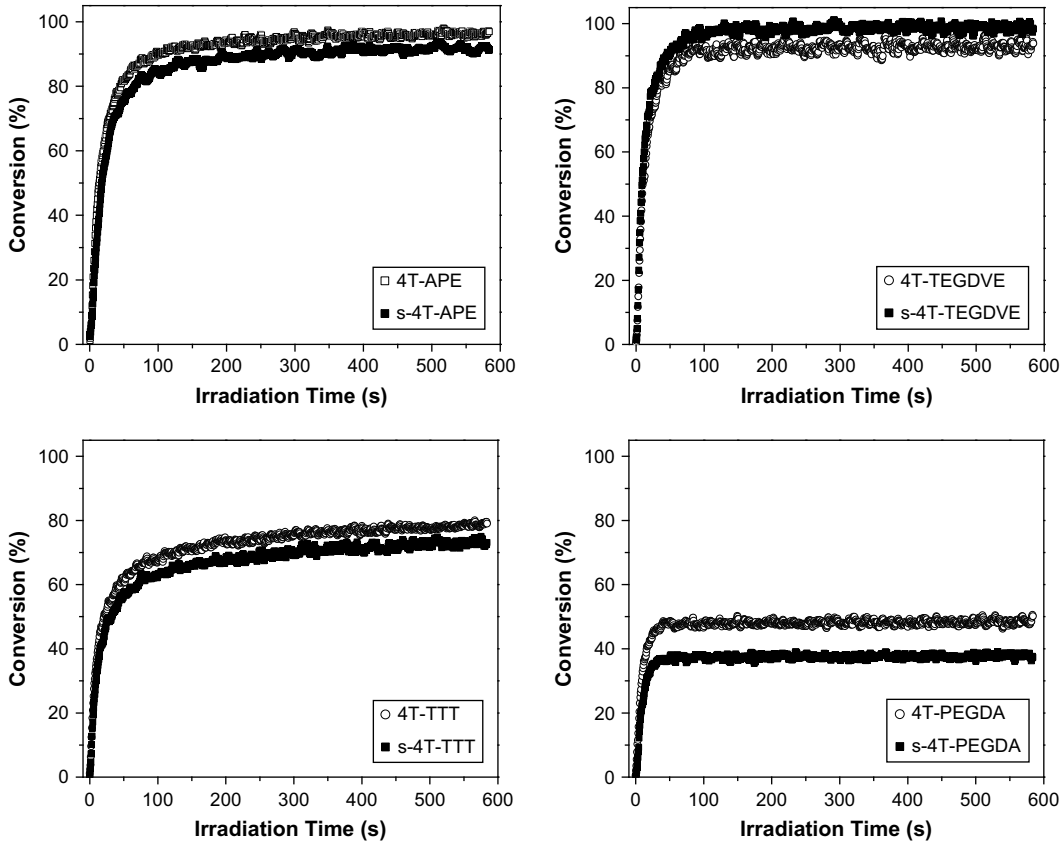

Fig. 1. Percent conversion of thiol group as a function of irradiation time (SH:C=C = 1:1 mol/mol). Light intensity = 0.625 mW/cm^2.

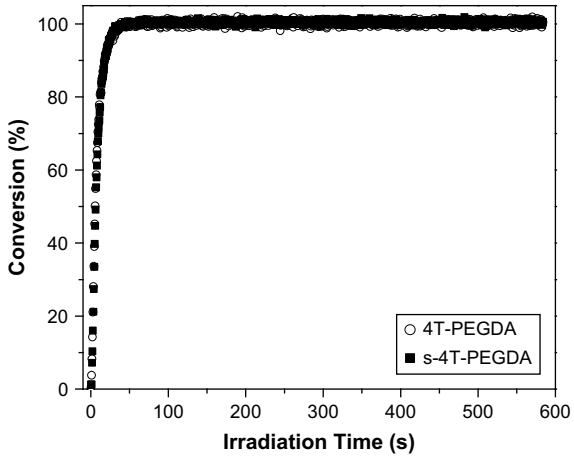

Fig. 2. Percent conversion of acrylate group as a function of irradiation time (SH:C=C = 1:1 mol/mol). Light intensity = 0.625 mW/cm^2.

[28]. To this end, we have prepared networks in formats where both the thermal and physical transitions can readily be evaluated, thus providing further critical information about the nature of chemical structural effects and monomer functionalilty on network properties. By including several types of basic ene structures along with structural changes in the thiol functional groups, i.e., primary and secondary, and providing thermal and physical measurements on all systems a clear venue for comparing directly structure–property relationships that effect the performance properties of thiol–ene networks is established. In the preparation of photocured films for physical property evaluation, except for cases where the TTT ene monomer was used, essentially complete conversions of the thiol–ene films were ensured by the experimental conditions used, i.e., 10 passes under the high-intensity Fusion lamp system (3.0 W/cm^{-2}) at a belt speed of 3.05 m/min. In the case of films produced from 1:1 molar functional group mixtures of 4T and s-4T with TTT, annealing subsequent to photocuring would be expected to lead to higher conversions, depending upon the exact conditions of irradiation and annealing since the inherent glass transition of the photocured network is much greater than room temperature. However, since the intention was to determine properties under typical photocuring conditions, no thermal annealing was performed for these networks. Additionally, no thermal annealing was performed for any of the other thiol–ene samples subsequent to photocuring. Of course, since the other networks have glass transitions less than room temperature, their typical limiting conversions were inherently much closer to quantitative under the photocuring conditions employed. The DSC scans and corresponding glass transition temperatures of the photocured thiol–ene networks prepared from samples with s-4T shown in Fig. 3 and Table 2 in most cases were marginally higher than the networks prepared from samples with 4T. These differences, which are quite small, could be due to hindered rotation of thiol–ether linkages (–S–) afforded by the additional α-methyl group of s-4T, or differences in purity of the 4T and s-4T samples. It is of interest to note that the 4T–TTT and s-4T–TTT networks have the same glass transition temperature; ostensibly this may be due to the glass

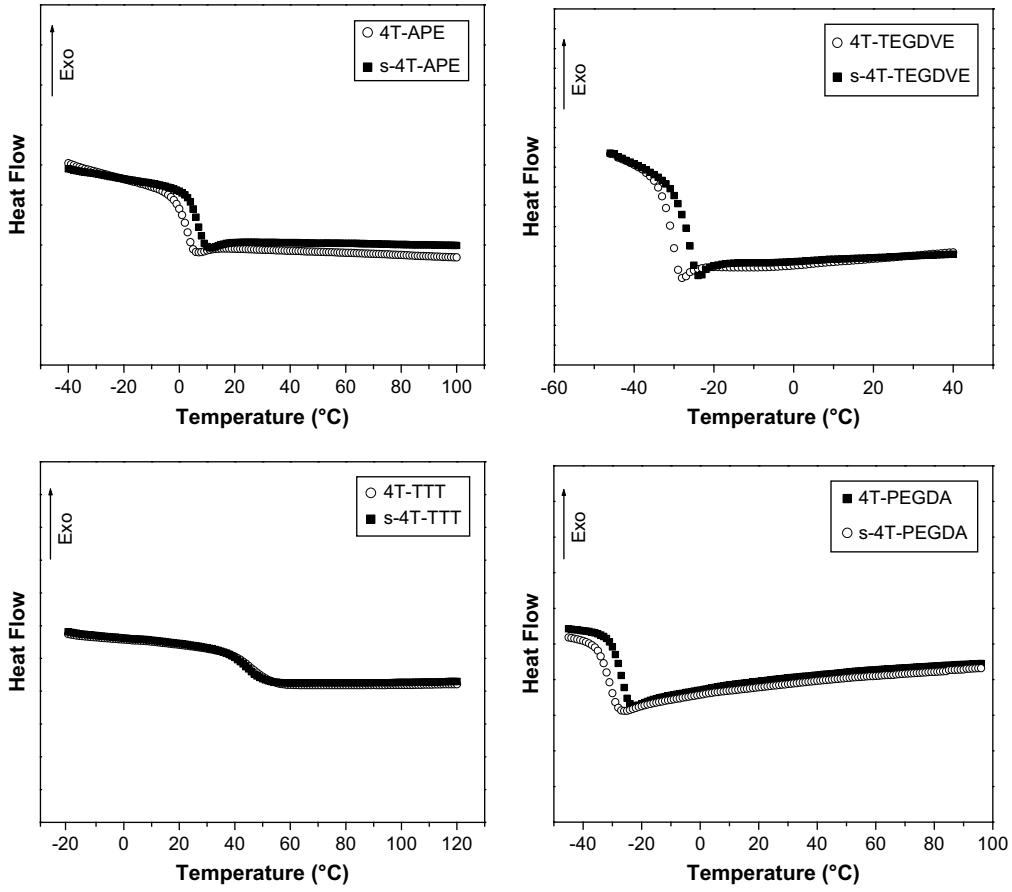

Fig. 3. DSC curves of thiol–ene networks measured at a heating rate of 10 °C/min.

Table 2
Glass transition temperature and heat capacity change of thiol–ene networks measured by DSC.

	APE		TEGDVE		TTT		PEGDA	
	4T	s-4T	4T	s-4T	4T	s-4T	4T	s-4T
T_g (°C)	3	7	−30	−25	45	45	−30	−26
ΔC_p (J/(g °C))	0.41	0.40	0.71	0.61	0.31	0.30	0.53	0.50

transition of both systems increasing during polymerization reaching the same limiting value in both cases. For both the s-4T and 4T based networks, the rigid TTT structure also provides the highest T_g for any of the enes, i.e., thiol–ene films based on the APE structures with flexible ether groups have much lower T_gs than the TTT based ones. The DSC T_g results for 4T–APE reported herein are in agreement with literature values [28]. The combined effect of lower network density via a lower ene functionality and more flexible chemical structure results in networks with very low T_gs for the TEGDVE (ene functionality of 2) and PEGDA (ene functionality of 2 with respect to the thiol reaction) based systems. In the case of thiol–ene networks formed from PEGDA, there are significant contributions from acrylate homopolymerization as already noted. The low T_g values obtained for the ether containing networks are consistent with the well recognized flexibility and low glass transitions of polymers containing ether linkages.

Next a particularly interesting phenomenon for the networks based on TEGDVE and PEGDA, which have more flexible structures and lower network densities, is assessed. From the DSC scans in Fig. 3, it is possible to measure the differences in heat capacities in the glass and rubbery states. It has been shown that the resulting specific heat capacity changes, ΔC_p, at the glass transition region are very important in assessing the propensity of thiol–ene networks to undergo rapid and efficient sub-T_g relaxation upon thermal annealing of the networks at temperatures just a few degrees below the glass transition measured by the second heating DSC scans [28]. By examining the effect of chemical structure on sub-T_g relaxation of thiol–ene networks, it was determined that the larger the ΔC_p value for a particular network, the greater will be the extent of sub-T_g relaxation. Interestingly, the ΔC_p value was found to decrease as the rigidity of the network increases and the crosslink density, determined by the functionality of the thiol and ene components, increases [28]. In the previous investigation, the highest ΔC_p value (0.56 J/(g °C)) for any thiol–ene network was for hexanedithiol and APE. In considering the results for the thiol–ene systems that are the subject of this investigation, it is first noted from the results in Table 2 that the ΔC_p values for the samples prepared from 4T and s-4T were not very different for a given multifunctional ene. Second, the changes in heat capacity at the glass transition are smallest for the trifunctional APE and TTT based networks due to the trifunctionality of these monomers, with the more rigid TTT based networks having the lowest ΔC_p values. In contrast to the networks formed from APE and TTT with s-4T and 4T, the ΔC_p values for 4T–TEGDVE and s-4T–PEGDVE, 0.71 J/(g °C) and 0.61 J/(g °C), respectively, are the largest values to date reported for a thiol–ene network [28]. Focusing on the s-4T–TEGDVE and 4T–TEGDVE systems which are true thiol–ene network unencumbered by homopolymerization of the ene, the high ΔC_p values reflect the increased propensity for molecular motion in the rubbery state afforded by the combination of a flexible polyether unit and low network crosslink density due to the difunctionality of TEGDVE. Elaborating, the restricted mobility in the glass phase of all of the pure thiol–ene networks means that the basic vibration and short scale motions for heat absorption are fairly consistent from

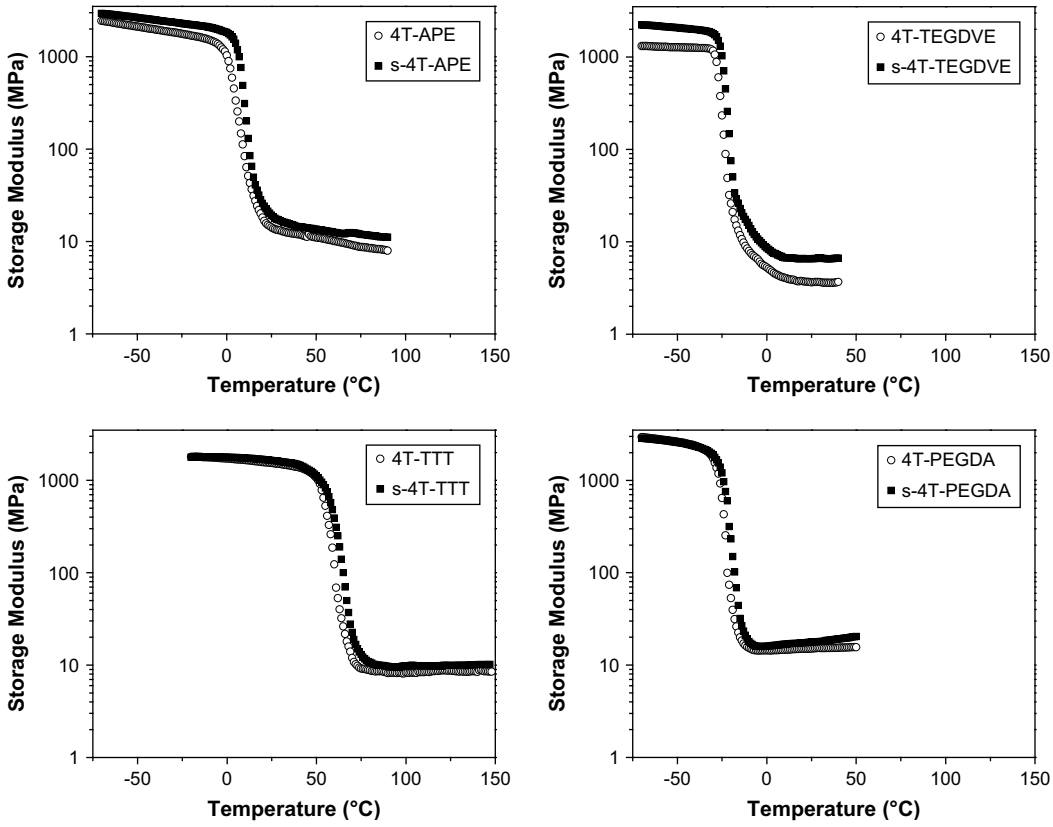

Fig. 4. E' of thiol–ene networks measured with DMA operating in tensile mode (3 °C/min, 1 Hz).

Table 3
Glass transition temperature of thiol–ene networks measured with DMA.

	APE		TEGDVE		TTT		PEGDA	
	4T	s-4T	4T	s-4T	4T	s-4T	4T	s-4T
T_g (°C)	8	13	−24	−20	63	64	−22	−17
E' at 23 °C (MPa)	15.3	20.0	4.0	7.2	1568.1	1658.0	15.2	18.1
E' at $T_g + 50$ °C (MPa)	10.3	12.2	3.9	6.6	8.4	9.8	15.2	18.1
FWHM (°C)	14	11	12	10	25	28	11	12

network to network, and hence in the glassy phase relatively independent of the crosslink density and basic rigidity of the chemical structural components. This is not the case in the rubbery phase where the network crosslink density and rigidity of the chemical structures will control the absorption of heat as temperature increases, i.e., the more flexible and lower crosslinked 4T–TEGDVE and s-4T–TEGDVE networks will have the highest heat capacities. Finally, the $\Delta C_p \times \Delta T$ value, where ΔT is taken as 10 °C reflecting a difference of 10 °C between the T_g and the sub-T_g aging temperature, suggests that the ultimate enthalpy relaxation value for the 4T–TEGDVE network should be 7.1 J/g.

To provide corroborative evidence for the DSC results and provide a conduit for interpretation of the Persoz results to follow, a DMA analysis of each of the photocured thiol–ene networks was conducted. The results in Fig. 4 for the E' versus temperature plots (see Experimental for details of sample preparation and scan) show a significant decrease in the storage modulus by about two orders of magnitude in each case as the sample experiences a distinct and narrow glass transition region. This is certainly consistent with the DSC results in Fig. 3 where increases in the heat capacity over a narrow temperature range were recorded. One noteworthy item

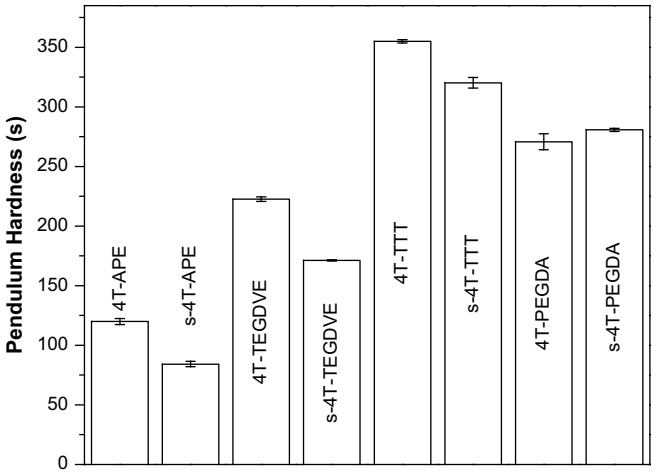

Fig. 6. Persoz pendulum hardness of thiol–ene networks.

in comparing the storage modulus values for the three purely thiol–ene networks is that the E' values for the s-4T–TEGDVE and 4T–TEGDVE systems were less than the E' values for the other thiol–ene networks in the rubber phase for a given temperature (values of E' at $T_g + 50$ °C are shown in Table 3) above the glass transition. This reflects the lower crosslink density for the s-4T–TEGDVE and 4T–TEGDVE networks resulting from the lower functionality of the ene component compared to the TTT and APE enes. The lower E' values for s-4T–TEGDVE and 4T–TEGDVE at $T_g + 50$ °C indicate a more loosely bound network with greater coordinated segmental motion

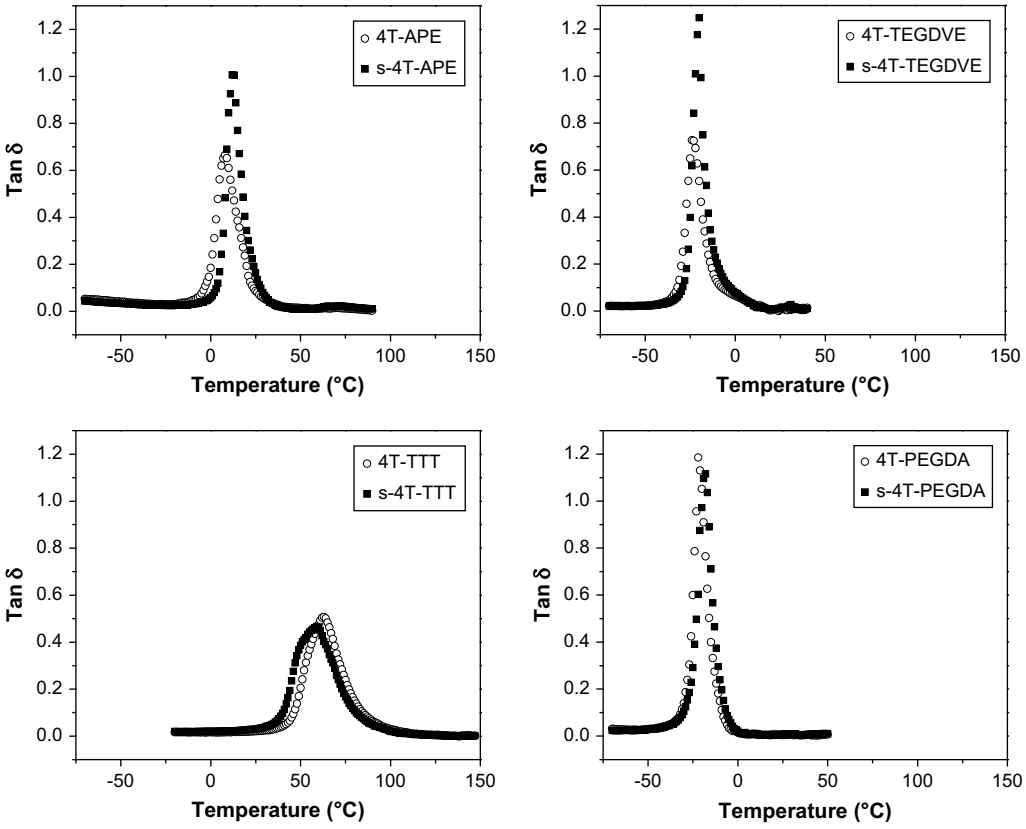

Fig. 5. tan δ of thiol–ene networks measured with DMA operating in tensile mode (3 °C/min, 1 Hz).

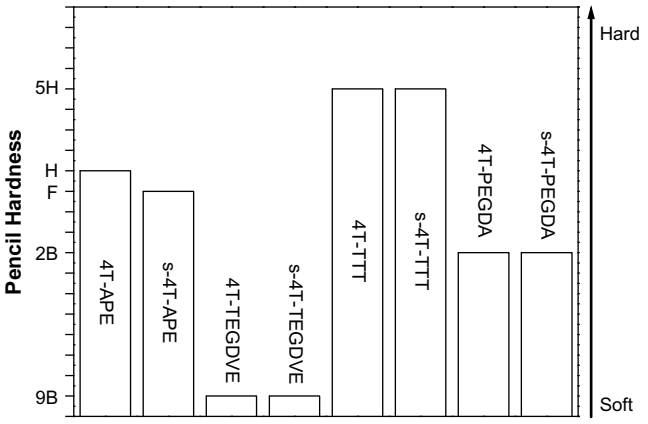

Fig. 7. Pencil hardness of thiol–ene films.

consistent with the higher ΔC_p values, reflecting the increased extent of coordinated chain mobility in the rubbery state compared to the more restricted s-4T–APE, 4T–APE, s-4T–TTT, and 4T–TTT networks.

Additional information about the glass transition region of the thiol–ene networks can be obtained from the DMA based tan δ versus temperature plots in Fig. 5. The temperatures at the peak maxima, taken as the glass transition temperatures, are listed in Table 3 for each of the networks. As found for the DSC results, the T_g values for networks made from the secondary thiol are slightly higher in most cases. The T_gs for the 4T–TTT and 4T–TEGDVE films, 63 °C and −24 °C, are consistent within 2–3 °C of the DMA based T_g values reported in the literature [29–33]. Consistent with previous reports in the literature for thiol–ene based networks [1], the full width at half maximum (FWHM) values for thiol–ene networks in this investigation, including the s-4T–PEGDA and 4T–PEGDA samples, are relatively low. The FWHM values are highly indicative of the uniformity of the network structures. Since the polymerizations of the s-4T–TEGDVE, 4T–TEGDVE, s-4T–APE and 4T–APE networks are conducted at temperatures well above the glass transition region, the very low FWHM values of 10–14 °C are the result of high, essentially quantitative conversions. The TTT based networks have the highest FWHM values, 25 and 28 °C. The broadness of these peaks as clearly seen in Fig. 5 arises, in part, from conversions which are not complete due to curing of samples that are initially at room temperature. Even though the samples increase in temperature during the photocuring process, the conversions are not optimized. Optimization of the conversions for such high T_g thiol–ene networks, including the 4T–TTT system, is currently being investigated and will be reported in a future publication focused on high density, high T_g thiol–ene networks.

The Persoz pendulum hardness of each thiol–ene network was also measured (Fig. 6). Any small differences between the primary and secondary thiol–ene networks are inconsequential and may arise from slight structural variations. The Persoz damping measurements can be conveniently interpreted in view of the DMA plots in Fig. 5. The TTT based networks are glassy at room temperature as indicated by the DMA tan δ results in Fig. 5 and have correspondingly negligible tan δ values. Hence, less

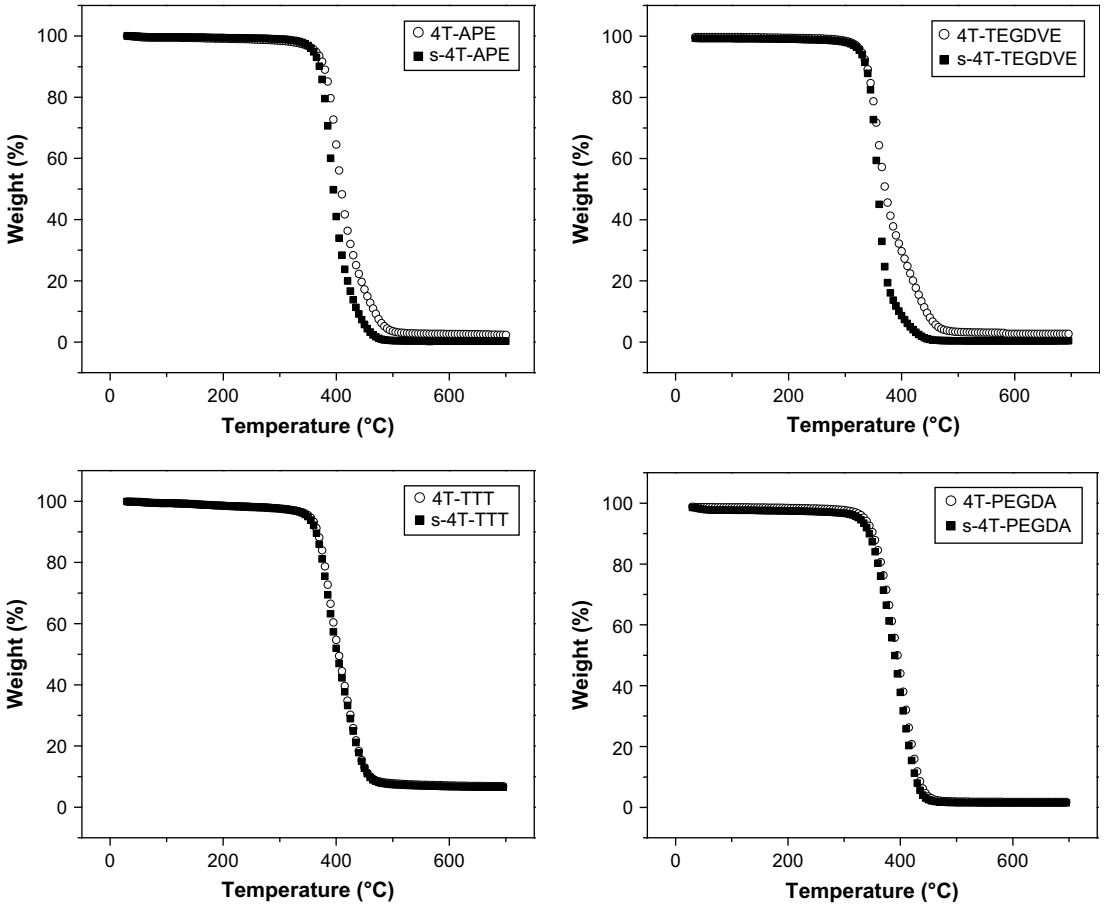

Fig. 8. TGA curves of thiol–ene films.

Table 4
Temperature at 5% weight loss ($T_{5\%}$) and temperature at the maximum degradation rate (T_{max}) of thiol–ene films.

	APE		TEGDVE		TTT		PEGDA	
	4T	s-4T	4T	s-4T	4T	s-4T	4T	s-4T
$T_{5\%}$ (°C)	362	360	328	326	352	350	332	330
T_{max} (°C)	400	390	358	357	388	386	403	400

energy is damped by the rigid glassy TTT based networks as attested to by the higher oscillation damping times (higher Persoz pendulum hardness values). The low damping times for the trifunctional APE based networks are consistent with the substantial tan δ values at room temperature (see curve in Fig. 5) where the Persoz damping measurements were made. The TEGDVE and PEGDA based films have higher oscillation damping times than for the APE networks since the Persoz measurements were made at room temperature (well above the glass transition region) where the tan δ values for these networks are very small.

Scratch resistance of network films is determined by many factors including network density and glass transition temperature. In all cases, the surface scratch resistances of the primary and secondary thiol–ene films measured are essentially identical (Fig. 7). As a result of their high network density, and the fact that they are glasses at room temperature, the TTT based films exhibit higher pencil hardness for both the 4T and s-4T based films. The lowest pencil hardness values are obtained for the films made using TEGDVE and PEGDA which have the lowest crosslink density and are rubbery at room temperature where the scratch resistance was measured. The thermal stability of all of the thiol–ene networks was measured by TGA heating at 10 °C/min in N_2; the weight loss curves are shown in Fig. 8 and the resultant 5% weight loss temperatures ($T_{5\%}$) and temperatures corresponding to the maximum weight loss (T_{max}) are listed in Table 4. Except for slight differences for the TEGDVE and APE based films at high temperatures, there are not any differentiable variations in thermal stability between primary and secondary based thiol–ene films. It is noted that the higher network crosslink densities for the TTT and APE based networks apparently help to stabilize the network structures at elevated temperature.

Finally, the refractive indices of all of the thiol–ene films were measured at ~24 °C. The relationship of the refractive index to other factors can be expressed by the Lorentz–Lorenz equation [34]

$$\frac{n^2-1}{n^2+2} = \frac{\rho N_{av}\alpha}{3M_0\varepsilon_0} \quad (1)$$

where n is the refractive index, ρ is the polymer density, α is the average polarizability, ε_0 is the vacuum permittivity, N_{av} is the Avogadro constant and M_0 is the polymer molecular weight. The dense glassy networks prepared from TTT exhibit the highest refractive index at 24 °C (Table 5). The low density and sulfur content of the PEGDA based networks lead to particularly low refractive index values.

Table 5
Refractive indices (±0.0001) of thiol–ene films.

	APE		TEGDVE		TTT		PEGDA	
	4T	s-4T	4T	s-4T	4T	s-4T	4T	s-4T
Refractive index	1.5350	1.5280	1.5215	1.5155	1.5622	1.5620	1.4906	1.4905
Sulfur content (wt%)	15.5	14.5	14.4	13.5	15.6	14.6	2.8	2.8

4. Conclusion

The photopolymerization of four different types of enes with primary and secondary thiol was investigated and physical and mechanical properties of the thiol–ene networks were measured. All ene monomers showed high reactivity with both thiols, with PEGDA homopolymerizing as well as copolymerizing with the thiol. The DSC and DMA results for each of the networks indicated narrow glass transition regions. The FWHM values ranged from 10 to 28 °C. Particularly high ΔC_p values were observed for the more flexible networks based on TEGDVE and both the primary and secondary tetra thiols. This was discussed in terms of enhanced heat capacity in the rubbery phase resulting from higher mobility provided by the lower crosslink density and very flexible ether groups incorporated into the network via the basic TEGDVE structure. The TTT based films with higher network crosslink densities and a rigid ene ring structure, generated films with higher glass transition temperatures, higher pencil hardness values and higher refractive indices. Persoz damping measurements were consistent with the DMA results and interpreted in terms of the value of the loss tangent at room temperature. Finally, all of the resin mixtures prepared from the commercial secondary thiol exhibited truly exceptional shelf-life compared to mixtures containing the primary thiol, and the secondary thiol sample evaluated had little or no objectionable odor making it particularly suitable for many applications.

Acknowledgement

This work was supported by the MRSEC Program of the National Science Foundation under Award Number DMR 0213883. We also acknowledge Fusion UV Systems, Inc. for curing units. The ene monomers were generously provided by Sartomer Chemical Company and Perstorp, while Showa Denko K.K. provided the secondary tetrathiol and Ciba Specialty Chemicals provided the photoinitiator.

References

[1] Hoyle CE, Lee TY, Roper T. Journal of Polymer Science, Part A: Polymer Chemistry 2004;42:5301.
[2] Katoh T, Kamata H, Onishi M. PCT Patent Application, WO03072614; 2003.
[3] Jacobine AF. In: Fouassier JD, Rabek JF, editors. Radiation curing in polymer science and technology III: polymerization mechanisms. London: Elsevier; 1993. p. 219–68.
[4] Gush DP, Ketley AD. Modern Paint and Coatings 1978, November;58.
[5] Cramer NB, Bowman CN. Journal of Polymer Science, Part A: Polymer Chemistry 2001;39:3311.
[6] Morgan CR, Magnotta F, Ketley AD. Journal of Polymer Science: Chemistry Edition 1977;15:627.
[7] Klemm E, Sensfuss S, Holfter U, Flammersheim HJ. Angewandte Makromolekulare Chemie 1993;212:121.
[8] Kuhne G, Diesen JS, Klemm E. Angewandte Makromolekulare Chemie 1996;242:139.
[9] Rehnberg N, Annby U, Sjorgreen CA, Davidson RS. PCT Patent Application, WO2001044377; 2001.
[10] Stahly EE. US Patent 3619393; 1971.
[11] Guthrie JL, Rendulic FJ. US Patent 3855093; 1974.
[12] Woods JG, Jacobine AF. RadTech NA Technical Conference Proceedings, vol. I; 1992. p. 173.
[13] Dowling JP, Richardson SC, Quigley K. US Patent 5358976; 1994.
[14] Rakas MA, Jacobine AF. Journal of Adhesion 1992;36:247.
[15] Kamata H, Onishi M. Japan Kokai Tokkyo Koho, JP2006151958; 2006.
[16] Ikeda H, Miyata H, Murofushi K. PCT International Application, WO2008023603; 2008.
[17] Miyata H, Ikeda H, Murofushi K, Hattori Y, Urakawa K. PCT International Application, WO2007145241; 2007.
[18] Murofushi K, Hattori Y. Japan Kokai Tokkyo Koho, JP2008013690; 2008.
[19] Okamoto M, Waki S, Mase H. Japan Kokai Tokkyo Koho, JP2008095035; 2008.
[20] Hisama S, Ichinohe D. Japan Kokai Tokkyo Koho, JP2008077067; 2008.
[21] Suzuki T. Japan Kokai Tokkyo Koho, JP2008065040; 2008.
[22] Yamauchi T, Ito H, Morishita S, Tani H. Japan Kokai Tokkyo Koho, JP2004325735; 2004.
[23] Takebe K. Faming Zhuanli Shenqing Gongkai Shuomingshu, CN101121825; 2008.

[24] Irie K, Ito H, Taguchi T, Kato T, Murofushi K. Japan Kokai Tokkyo Koho, JP2003252918; 2003.
[25] Clark T, Kwisnek L, Hoyle CE, Nazarenko S. Journal of Polymer Science, Part A: Polymer Chemistry 2008;47:14–24.
[26] Zhou H, Li Q, Lee TY, Guymon CA, Johnsson ES, Hoyle CE. Macromolecules 2006;39:8269.
[27] Wei H, Li Q, Ojelade M, Madbouly S, Otaigbe JU, Hoyle CE. Macromolecules 2007;40:8788.
[28] Shin J, Nazarenko S, Hoyle CE. Macromolecules 2008;41:6741.
[29] Cook WD, Chausson S, Chen F, Pluart LL, Bowman CN, Scott TF. Polymer International 2008;57:469.
[30] Cook WD, Chen F, Pattison DE, Hopson P, Beaujon M. Polymer International 2007;56:1572.
[31] Carioscia JA, Schneidewind L, O'Brien C, Ely R, Feeser C, Cramer N, et al. Journal of Polymer Science, Part A: Polymer Chemistry 2007;45:5686.
[32] Li Q, Zhou H, Wicks DA, Hoyle CE. Journal of Polymer Science, Part A: Polymer Chemistry 2007;45:5103.
[33] Lu H, Carioscia JA, Stansbury JW, Bowman CN. Dental Materials 2005; 21:1129.
[34] Mills NJ. In: Mark HF, Bikales NM, Overberger CG, Menges G, Kroschwitz JI, editors. Encyclopedia of polymer science and engineering. 2nd ed., vol. 10. New York: John Wiley and Sons; 1987. p. 493–540.